(12)

AFGL-TR-85-0200
ENVIRONMENTAL RESEARCH PAPERS, NO. 926

AD-A164 424

Model Vertical Profiles of Extreme Rainfall Rate, Liquid Water Content, and Drop-Size Distribution

PAUL TATTELMAN
PAUL T. WILLIS

6 September 1985

ATMOSPHERIC SCIENCES DIVISION PROJECT 6670
AIR FORCE GEOPHYSICS LABORATORY
HANSCOM AFB, MA 01731

This report has been reviewed by the ESD Public Affairs Office (PA) and is releasable to the National Technical Information Service (NTIS).

"This technical report has been reviewed and is approved for publication"

FOR THE COMMANDER

DONALD D. GRANTHAM
Chief, Atmospheric Structure Branch

ROBERT A. McCLATCHEY
Director, Atmospheric Sciences Division

Qualified requestors may obtain additional copies from the Defense Technical Information Center. All others should apply to the National Technical Information Service.

If your address has changed, or if you wish to be removed from the mailing list, or if the addressee is no longer employed by your organization, please notify AFGL/DAA, Hanscom AFB, MA 01731. This will assist us in maintaining a current mailing list.

Do not return copies of this report unless contractual obligations or notices on a specific document requires that it be returned.

Unclassified

SECURITY CLASSIFICATION OF THIS PAGE

AD-A164424

REPORT DOCUMENTATION PAGE

1a. REPORT SECURITY CLASSIFICATION: Unclassified	1b. RESTRICTIVE MARKINGS
2a. SECURITY CLASSIFICATION AUTHORITY	3. DISTRIBUTION/AVAILABILITY OF REPORT: Approved for public release; distribution unlimited.
2b. DECLASSIFICATION/DOWNGRADING SCHEDULE	
4. PERFORMING ORGANIZATION REPORT NUMBER(S): AFGL-TR-85-0200 ERP, No. 928	5. MONITORING ORGANIZATION REPORT NUMBER(S)
6a. NAME OF PERFORMING ORGANIZATION: Air Force Geophysics Laboratory; 6b. OFFICE SYMBOL (If applicable): LYA	7a. NAME OF MONITORING ORGANIZATION
6c. ADDRESS (City, State and ZIP Code): Hanscom AFB Massachusetts 01731-5000	7b. ADDRESS (City, State and ZIP Code)
8a. NAME OF FUNDING/SPONSORING ORGANIZATION; 8b. OFFICE SYMBOL (If applicable)	9. PROCUREMENT INSTRUMENT IDENTIFICATION NUMBER
8c. ADDRESS (City, State and ZIP Code)	10. SOURCE OF FUNDING NOS.

PROGRAM ELEMENT NO.	PROJECT NO.	TASK NO.	WORK UNIT NO.
62101F	6670	09	11

11. TITLE (Include Security Classification) Model Vertical Profiles of Extreme Rainfall Rate, (Contd)

12. PERSONAL AUTHOR(S): Paul Tattelman and Paul T. Willis*

13a. TYPE OF REPORT	13b. TIME COVERED	14. DATE OF REPORT (Yr., Mo., Day)	15. PAGE COUNT
Scientific-Final	FROM 1984 TO 1985	1985 September 6	42

16. SUPPLEMENTARY NOTATION

*Atlantic Oceanographic and Meteorological Laboratory; 4301 Rickenbacker Causeway, Miami, Florida 33149

17. COSATI CODES		
FIELD	GROUP	SUB. GR.

18. SUBJECT TERMS (Continue on reverse if necessary and identify by block number)

Rainfall rate; Hydrometeors; Liquid water content; Rainfall extremes; Drop-size distribution; Climatic extremes

19. ABSTRACT (Continue on reverse if necessary and identify by block number)

This report provides a new model of hydrometeors and associated cloud-water content from the surface to 20 km. The model profiles at altitude were developed based on five surface rainfall rates: 36, 84, 168, 432, and 1872 mm/hr. The first three rates correspond to a frequency of occurrence of 0.5 percent, 0.1 percent, and 0.01 percent of the time during the worst month in the most severe area of the world for intense rainfall. The last two are the 42- and 1-min world record rainfalls. The surface rainfall rates were extrapolated aloft using results from previous studies.

A large sample of drop-size distributions from intense rainfall collected during reconnaisance of Atlantic hurricanes/tropical storms was analyzed. The data set was normalized and fit by a gamma distribution. This was used to specify the drop-size distributions and liquid water content for rainfall rates specifies at the surface and aloft. Concurrent cloud-water content was estimated. Results are presented at 2-km intervals.

20. DISTRIBUTION/AVAILABILITY OF ABSTRACT	21. ABSTRACT SECURITY CLASSIFICATION
UNCLASSIFIED/UNLIMITED ☐ SAME AS RPT. ☒ DTIC USERS ☐	Unclassified

22a. NAME OF RESPONSIBLE INDIVIDUAL	22b. TELEPHONE NUMBER (Include Area Code)	22c. OFFICE SYMBOL
Paul Tattelman	(617) 861-5957	LYA

DD FORM 1473, 83 APR EDITION OF 1 JAN 73 IS OBSOLETE.

Unclassified

SECURITY CLASSIFICATION OF THIS PAGE

11. (Contd)

Liquid Water Content, and Drop-Size Distribution

Preface

The authors are grateful to Major Al Boehm, AFGL for his helpful suggestions, to Ms. Joyce O. Berkeley, NOAA, for reducing the rain rate data, and to Mrs. Helen Connell, AFGL, for typing this report.

Contents

Illustrations

Tables

Tables

Model Vertical Profiles of Extreme Rainfall Rate, Liquid Water Content, and Drop-Size Distribution

1. INTRODUCTION

This report provides a new model profile of hydrometeors and associated cloud-water content from the surface to 20 km. The model profiles at altitude are associated with specified extreme surface rainfall rates. Extremes of hydrometeors at the surface and aloft affect the design and operation of many aerospace systems due to the high potential for damage, or equipment failure, caused by impact with precipitation particles. Whereas extremes of some elements (for example, atmospheric density) only cause reduced performance, hydrometeor extremes (water and ice) can create excessive cooling in jet engines resulting in flameout and failure, or they can cause damage to engine turbine blades. Other effects include erosion on leading edges of aircraft or helicopter rotor blades, ablation of reentry vehicles, and triggering of impact fuses on airborne ordnance. Rainfall rates are important considerations for communication systems using microwave frequencies (for example, satellite systems) due to attenuation of signals. High rainfall rates can also cause leakage into sealed components such as electronic devices. Realistic profiles of hydrometeor extremes are needed for these and other design considerations important to the AF and other DoD agencies, and will be included in the revision of MIL-STD-210B, "Climatic Extremes for Military Equipment."[1]

(Received for publication 5 September 1985)

1. Department of Defense (1973) Military Standard, Climatic Extremes for Military Equipment, MIL-STD-210B, 15 December 1973, Office of the Under Secretary of Defense, Research and Engineering, Washington, D. C.

Studies of hydrometeor extremes up to 20 km altitude were done for MIL-STD-210B by Sissenwine,[2] and Tattelman and Sissenwine.[3] These studies present rainfall rates and associated liquid water content (LWC) and drop-size distribution at 0, 1, and 2 km and at 2-km intervals thereafter up to 20 km. The rates aloft are based on estimates of rainfall rates at the surface occurring 0.1 and 0.5 percent of the time during the worst month in the severest rain areas of the world,[4] and on world record 1- and 42-min rainfall rates.

Rainfall rates were calculated at altitude by Sissenwine using limited information on the vertical distribution of rainfall rates. He used these data to determine ratios of the rate aloft to that at the surface. These ratios were then applied to the 0.1 and 0.5 percent worst month, and 1- and 42-min world record surface rates. Associated LWC and drop-size distributions were determined using an empirical exponential relationship for convective heavy rain situations.

Recent work on a model for estimating 1-min rain rates by Tattelman and Scharr[5] indicates that values previously estimated by Salmela et al were too high. Furthermore, the ratios used by Sissenwine produced the highest rainfall rates aloft with a maximum at about 4.5 km. Current evidence contradicts this scenario when high rates have reached the surface. Finally, LWC calculated from the exponential relationship with rainfall rate produced different values from those arrived at by manually integrating the associated drop-size distributions.

This report provides more realistic profiles, than the above studies, by utilizing a unique data source analyzed by the NOAA/Atlantic Oceanographic and Meteorological Laboratory/Hurricane Research Division. This source contains high-intensity rain rates observed during aircraft research and reconaissance of Atlantic Hurricanes and tropical storms.

2. SURFACE RAINFALL RATES

The distribution of hydrometeors aloft specified in MIL-STD-210B is assumed to be associated with the surface rainfall rate. In this way, the entire profile can

---

2. Sissenwine, N. (1972) Extremes of Hydrometeors at Altitude for MIL-STD-210B, AFCRL-TR-72-0369, AD 747482.

3. Tattelman, P., and Sissenwine, N. (1973) Extremes of Hydrometeors at Altitude for MIL-STD-210B, Supplement Drop-size Distributions, AFCRL-TR-73-0008, AD 756832.

4. Salmela, H.A., Sissenwine, N., and Lenhard, R.W. (1971) Preliminary Atlas of 1.0, 0.5, and 0.1 Percent Precipitation Intensities for Eurasia, AFCRL-TR-71-0527, AD 736408.

5. Tattelman, P., and Scharr, K.G. (1983) A model for estimating one-minute rainfall rates, J. of Climate and Appl. Meteor. 22:1575-80.

be assigned the frequency of occurrence associated with the surface rate, for which far more data are available. This rationale is also used for the model profiles derived herein.

2.1 Frequencies of Extreme Rates

During the preparation of MIL-STD-210B, the Office of the Assistant Secretary of Defense specified that the frequency of occurrence during the worst month in the severest part of the world for a climatic element should be the basis for values presented in the Standard. For rainfall and associated vertical profiles, rates occurring 0.5 and 0.1 percent of the time in southeastern Asia are provided in 210B. Rates and profiles for the 1-min and 42-min world records are also provided.

Salmela et al[4] determined the 0.5 and 0.1 percent surface rates to be 0.8 mm/min (48 mm/hr) and 3.13 mm/min (188 mm/hr), respectively. The estimates were based on a model that was considered preliminary, but was the best available to provide inputs for the Standard. Subsequent modeling of 1-min rates by Tattelman and Scharr[5] indicate that the previous estimates were too high. This overestimate was primarily caused by the use of questionable data from Bogor, Indonesia, which caused a bias towards high estimates in the tropics. For Cherrapunji, India, at about 1300 m elevation, acknowledged as the world s rainiest location, the previous model estimated a 0.5 percent worst month value of 1.50 mm/min. The new model estimate is 0.61 mm/min. For Quang-tri, Indochina, the estimates for 0.5 percent are 0.79 and 0.39 mm/min, respectively, for the old and new models.

Atlases of 1-min rates,[6,7] based on the new model, were used to determine the areas in the world with the highest rainfall rates occuring 0.5, 0.1, and 0.01 percent of the time during the worst month. Although rates are generally highest in the northern hemisphere tropics, the estimated rates for two locations in northeast Brazil, Barro Do Corda and Teresina, are about the same as the rates estimated for Cherrapunji for all three frequencies. The rates for this area in northeast Brazil are 0.6 mm/min (36 mm/hr), 1.4 mm/min (84 mm/hr), and 2.8 mm/min (168 mm/hr) for 0.5, 0.1, and 0.01 percent of the worst month, respectively.

Elsewhere, values in the Northern Hemisphere tropics exceed 0.4, 1.2, and 2.4 mm/min during 0.5, 0.1, and 0.01 percent of the most severe month in many areas, especially in Southeast Asia. Since these rates occur over large areas in the tropics, the slightly higher rates in northeastern Brazil are recommended as representing the worst month/area rates.

---

6. Tattelman, P., and Grantham, D.D. (1983) Northern Hemisphere Atlas of 1-Min Rainfall Rates, AFGL-TR-83-0267, AD A145411.

7. Tattelman, P., and Grantham, D.D. (1983) Southern Hemisphere Atlas of 1-Min Rainfall Rates, AFGL-TR-83-0285, AD A145421.

The 1- and 42-min world record rates are 31.2 mm/min (1872 mm/hr), and 7.2 mm/min (432 mm/hr), respectively. These values were presented in MIL-STD-210B to provide guidance on the most extreme conditions observed. Model hydrometeor profiles for these surface rates are also derived in this report.

2.2 Effect of Downdrafts on Surface Rainfall Rate

The world record 1-min rainfall rate of 1872 mm/hr, measured at Unionville, Maryland, 4 July 1956, although a thoroughly investigated phenomenon, is still a little puzzling because it is almost twice as high as the next several candidates. Extreme rainfall rates tend to be self-limiting, because the collision breakup process effectively limits the maximum drop sizes that can be obtained. Further, the terminal velocities of large drops reach an asymptotic maximum at a diameter of 4 to 5 mm. So, the rainfall rate at extreme values has to be nearly directly proportional to liquid water content. And, although convergence can create, locally, very high liquid water contents, turbulent mixing will tend to limit the extreme maxima. Consequently, when a record rainfall is two times the next highest value, and all of the other record rates tend to cluster at about the same value, some other mechanism may be involved.

One possibility is the enhancement of surface rainfall rate by downdraft velocity. Although downdrafts are usually associated with the evaporation of precipitation, and thus are not usually coincident with extreme precipitation rates, it is entirely possible for very high precipitation rates to be associated with moderate downdrafts of 10-15 m/s. These could be in close proximity to very strong downbursts. At any rate, a moderate downdraft velocity could well be associated with high rainfall rate.

A moderately strong downdraft of only 10 m/s can double the surface rainfall rate. For example, assume that the near-record rainfall rate is about 900 mm/hr (15 mm/min) and that the associated water content, according to empirical relationships, is 30 g/m^3. A 10 m/sec downdraft superimposed on the fall velocities of the raindrops would increase the rainfall rate to 1980 mm/hr. This effect may well be involved in some gauge-measured record rainfalls. This effect would not be present in the aircraft-measured spectra of this study, nor in the Illinois drop camera measurements discussed later, because the cameras look at a fixed volume of air, not a flux of water through a plane surface, as in the case of a rain gauge.

The common downdraft velocity of only 2 m/sec can increase the gauge-measured rainfall of our example by 216 mm/hr, or about 20 percent. This effect should be considered in the interpretation of record rainfall events.

3. HYDROMETEORS ALOFT

3.1 Instrumentation and Data

The new data used to specify distributions aloft were collected in hurricanes and tropical storms by a P.M.S. optical spectrometer system described by Knollenberg.[8] Although the three probes of the system were usually operated, the data contained herein were obtained with the precipitation probe, which uses a 32-element photodiode array that covers diameters of 100-6500 μm with 200 μm resolution, or spacing, between elements. We present data from 10-sec summations, which cover horizontal distances of from 0.9 to 1.5 km, depending on the aircraft used and the altitude flown. Ordinarily the 10-sec sample encompasses a volume of about 2 cubuc meters. The data were objectively machine-reduced, using software described by Jorgensen and Willis.[9] The data sample analyzed was collected in tropical storms and hurricanes that occurred from 1975-1982. The high-intensity rainfall data used in this study were taken from about 14,000 10-sec aircraft samples in rain ($R > 0$).

The bulk of the data were sampled at two altitudes, 450 m and 3000 m. A small sample was obtained at two additional altitudes, one at 150 m, and one between the two primary sampling altitudes at 1500 m.

Blanchard and Spencer,[10] in surveying the availability of high rainfall rate drop size distribution data, conclude that, in spite of the many investigations of drop size distributions, only those by Mueller and Sims,[11] and Hudson,[12] include extensive data at intensities > 100 mm/hr. To determine drop-size distributions for this study, the new high rainfall rate data collected in hurricanes and tropical storms was used to fit a gamma function. The results are compared with the Mueller and Sims data. These were taken with a drop camera for 1-year periods at several locations around the world. The cubic meter samples, each covering 10.5 sec, were taken at 1-min intervals.

3.2 Drop-Size Distributions

3.2.1 THE GAMMA DISTRIBUTION

Most functional descriptions of the size distribution of raindrops are encompassed by the following expression:

$$N(D) = N_o D^{\alpha} \exp(-\Lambda D) \quad 0 < D < Dmax, \tag{1}$$

which is the gamma distribution function.[13] Here D is the drop diameter (N(D)dD is the concentration of drops having diameters between D and D+dD), Λ is the slope

---

(Due to the large number of references cited above, they will not be listed here. See References, page 33.)

parameter, and α is the shape parameter of the distribution. For the case where $\alpha = 0$ and $N_o = 0.08/cm^4$ this reduces to the familiar Marshall-Palmer exponential distribution.

It can be shown that D_o, the median volume diameter of a distribution, is given by the approximate expression

$$D_o = \frac{3.67 + \alpha}{\Lambda} \tag{2}$$

as long as $\alpha > -2$, and if $D_{max}/D_o > 2.5$. By straightforward integration, the following expressions for water content, M, and radar reflectivity factor, Z, can be derived. When a simple power law relation for the terminal velocity of the drops,

$$v = aD^b \tag{3}$$

is assumed (a = 1420 and b = 0.5 are often used), an expression for rainfall rate R can be derived as well:

$$M = \frac{\pi}{6} \rho_w \int_o^\infty N(D)D^3 dD = \frac{\pi}{6} \rho_w \frac{N_o \Gamma(\alpha + 4)}{\Lambda^{\alpha + 4}} \tag{4}$$

$$Z = \int_o^\infty N(D)D^6 dD = \frac{N_o \Gamma(\alpha + 7)}{\Lambda^{\alpha + 7}} \tag{5}$$

$$R = \frac{\pi}{6} a \int_o^\infty N(D)D^b D^3 dD = \frac{\pi}{6} a \frac{\Gamma(\alpha + b + 4)}{\Lambda^{\alpha + b + 4}} \tag{6}$$

where Γ is the gamma function.

Since several hundred individual spectra cannot be presented here, the data were stratified by four rainfall rate categories (25-62.5, 62.5 - 125, 125 - 225, and > 225 mm/hr) and two sampling altitudes (0.45 and 3 km). Then they were bin-averaged for each 0.2-mm-diameter interval. The resultant drop size distributions are shown for the entire data set stratified by rainfall rate in Figure 1. Also plotted in Figure 1 is a gamma distribution function fit, which will be discussed subsequently. The data for the two primary sampling altitudes, using the same rate stratification, is presented in Figures 2 and 3 (no data for rates > 225 mm/hr in Figure 2). Note that the 0.45 km sample exhibits a bimodality in the middle drop size diameters.

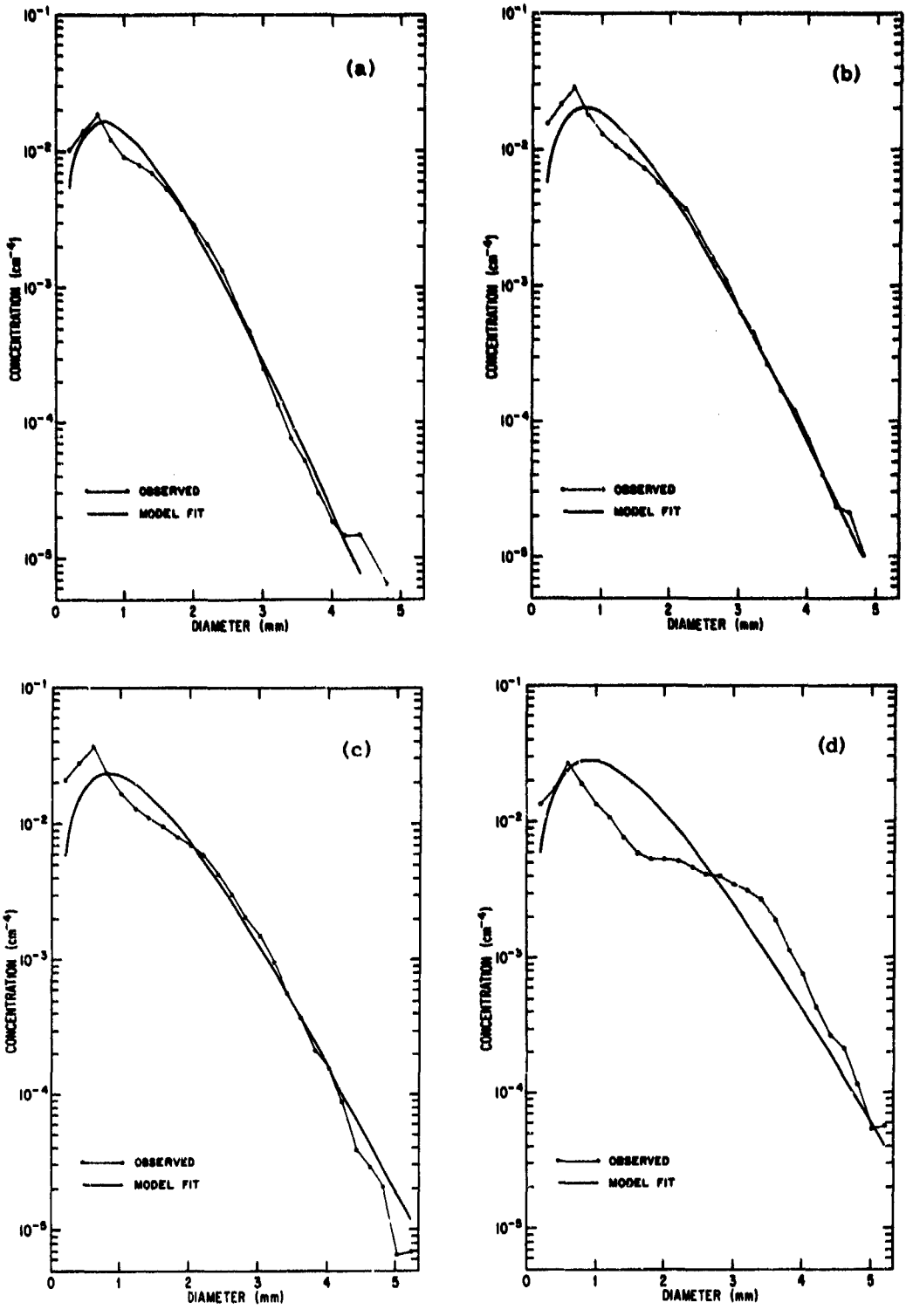

Figure 1. Drop-size Distribution for Observations at All Altitudes, and Gamma Function Fit for Rain Rates: (a) 25 to 62.5 mm/hr, (b) 62.5 to 125 mm/hr, (c) 125 to 225 mm/hr, and (d) > 225 mm/hr

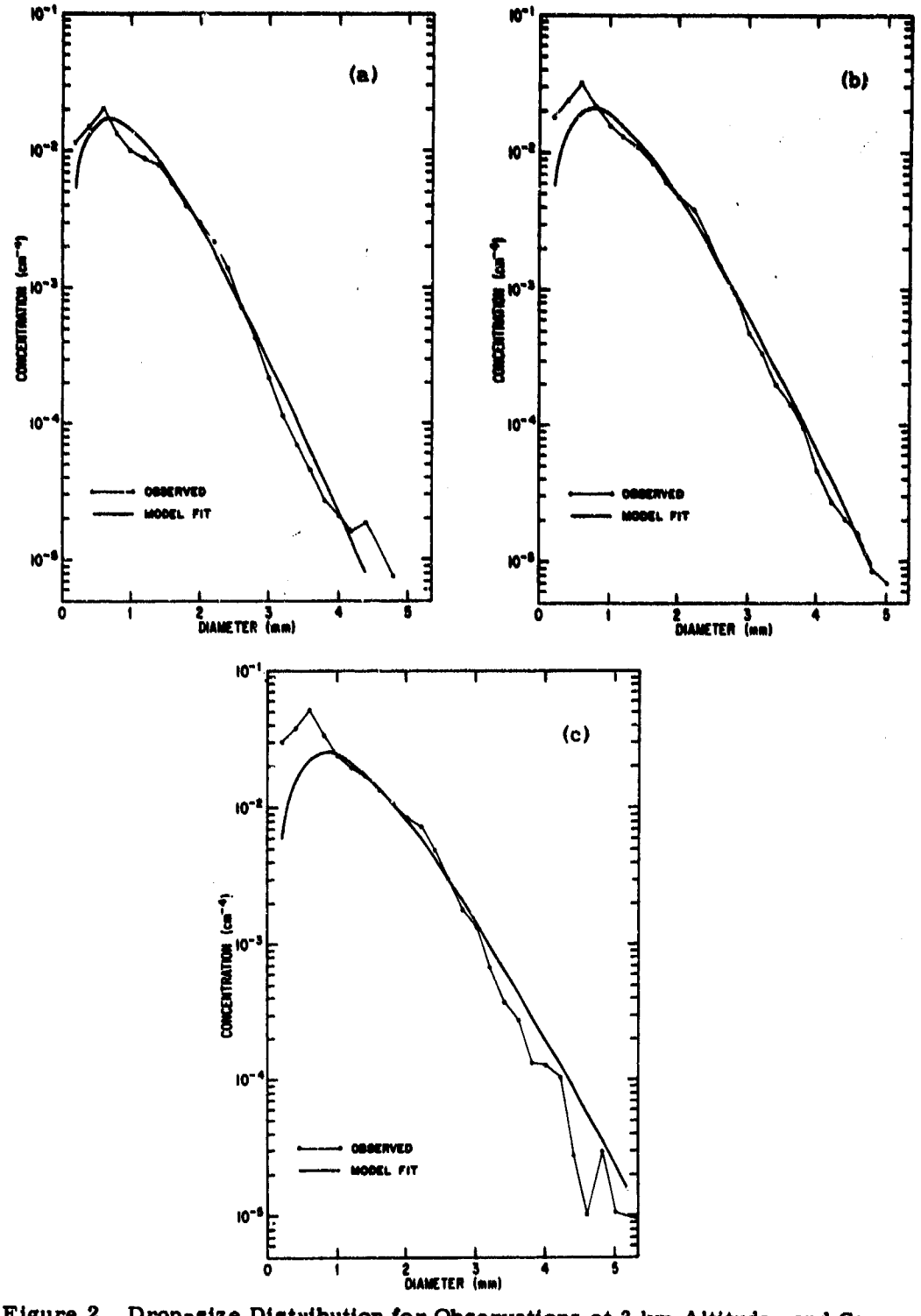

Figure 2. Drop-size Distribution for Observations at 3 km Altitude, and Gamma Function Fit for Rain Rates: (a) 25 to 62.5 mm/hr, (b) 62.5 to 125 mm/hr, and (c) 125 to 225 mm/hr

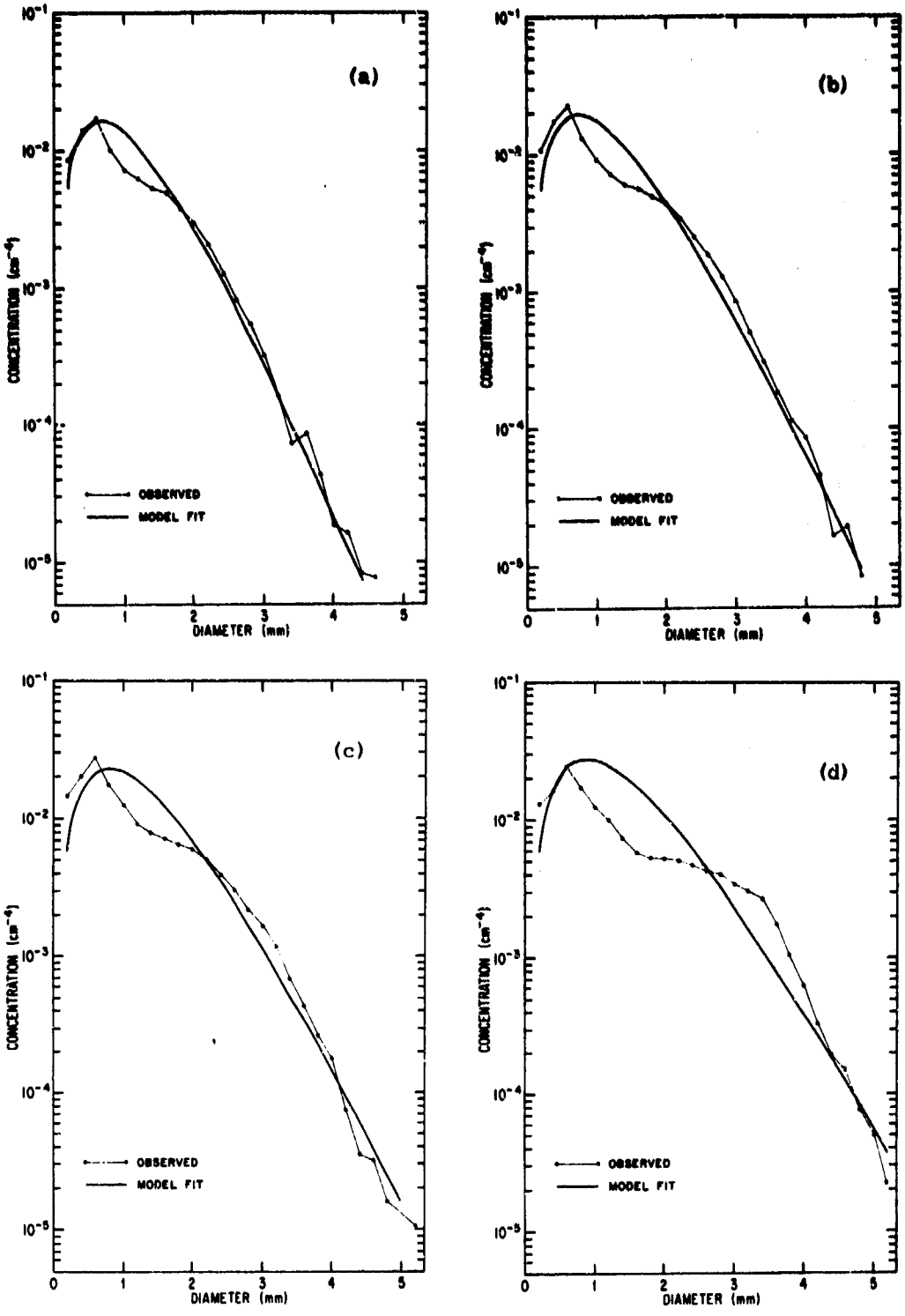

Figure 3. Drop-size Distribution for Observations at 0.45 km Altitude, and Gamma Function Fit for Rain Rates: (a) 25 to 62.5 mm/hr, (b) 62.5 to 125 mm/hr, (c) 125 to 225 mm/hr, and (d) > 225 mm/hr

Blanchard and Spencer[10] have indicated that a given intensity in heavy rain might correspond to a particular drop-size distribution, where drop growth is balanced by drop breakup. They hypothesize that the drop-size distribution in heavy rain is the same whether it originates from marine shower clouds or continental thunderstorms. They found that as the rain intensity exceeded 100 mm/hr, the largest drops in the distributions did not continue to increase in size relative to the smaller drops. Instead, as the rain intensity continued to increase, the total number of drops continued to increase. In our data from flight levels well below the freezing level we do not find extremely large diameter drops at the very high rainfall rates. There is some indication that, at the highest rates, the maximum sizes attained stabilize, or even decrease slightly. The large drops are difficult to observe adequately because of their low concentrations and the small spatial scale of high-intensity rain. However, for high-intensity rain we definitely observe significantly lower concentrations of drops of D > 4 mm than the concentrations indicated by the Marshall-Palmer distributions for these high rainfall rates.

The drop-size distributions presented in MIL-STD-210B are based on an exponential model of drop number concentrations. Numerous investigators have pointed out the inadequacies of the exponential distribution in describing observed drop-size distributions (for example, Ulbrich[13]), particularly for high-intensity convective rains. The gamma distribution function, of which the exponential is a special case, fits tropical convective rain distributions particularly well.[14] When the curvature parameter in Eq. (1), α, is zero, the gamma becomes the exponential distribution function.

The entire set of high-intensity rainfall data was normalized after the method of Sekhon and Srivastava[15, 16] to remove dependence of the distribution on water content or rainfall rate. The plot of all of the high-rate normalized data is shown in Figure 4. The data points are tightly grouped in the middle range of drop diameters. A curvilinear least-squares fit routine is then used to fit to the entire set of data points for rainfall rate > 25 mm/hr (N = 4624 points). The drop size distribution model consists of the equation for this normalized gamma function curve and an empirically determined relationship between water content, M, and median volume diameter, D_o, as described by Willis.[14] To fit an individual distribution, all that need be specified is the water content, M (or the rainfall rate, R). The fit to an individual distribution is determined by a denormalization of the fit to the entire normalized sample.

---

14. Willis, P. T. (1984) Functional fits to some observed drop size distributions and parameterizations of rain. J. Atmos. Sci. 41:1648-1661.

15. Sekhon, R. S., and Srivastava, R. C. (1970) Snow size spectra and radar reflectivity, J. Atmos. Sci. 27:299-307.

16. Sekhon, R. S., and Srivastava, R. C. (1971) Doppler observations of drop size distributions in a thunderstorm. J. Atmos. Sci. 28:983-994.

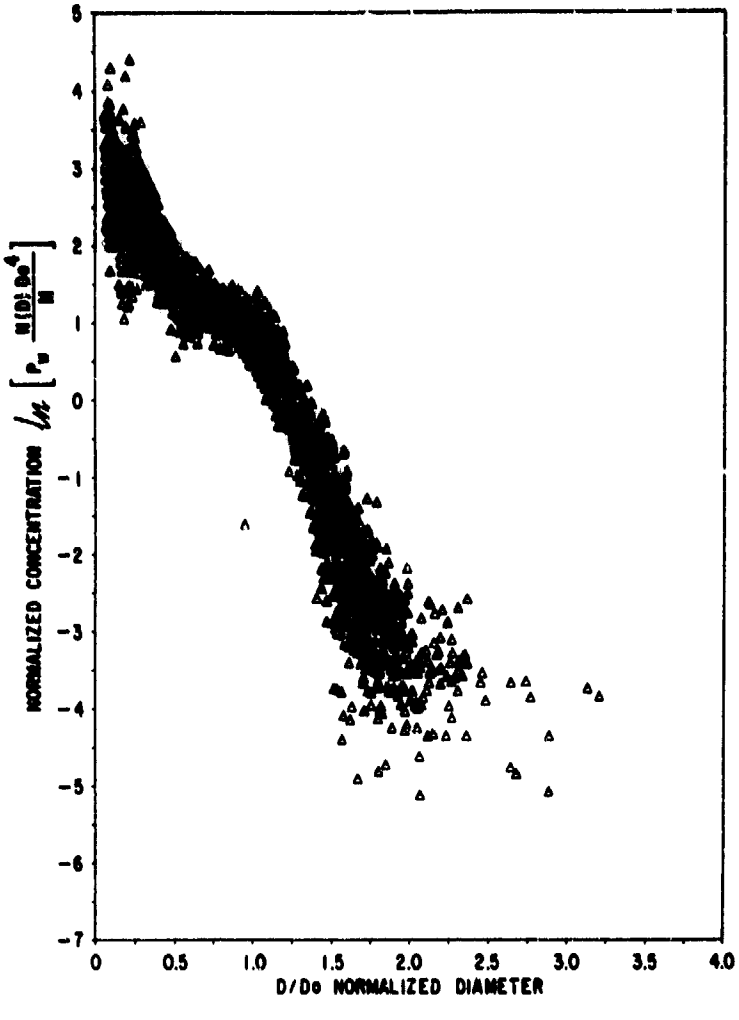

Figure 4. Normalized Distribution of the Total Data Sample

The model is applied as follows, if a drop-size distribution is desired for a given liquid water content M (g/m^3), first compute the median volume diameter from

$$D_o = 0.1571\ M^{0.1681} \tag{7}$$

where D_o is in cm. If the rainfall rate, R (mm/hr) is specified, compute M from

$$M = 0.062\ R^{0.913}\ . \tag{8}$$

Then the three parameters of the gamma distribution, Eq. (1), needed for the model are computed:

$$\Lambda = 5.5880/D_o \tag{9}$$

$$\alpha = 2.160 \tag{10}$$

$$N_o = \frac{512.85\ M \times 10^{-6}}{D_o^4} \left(\frac{1}{D_o}\right)^{2.160} . \tag{11}$$

The fit for a rainfall rate of 188 mm/hr is plotted in Figure 5. Also plotted in this figure, for comparison, is the appropriate Marshall-Palmer distribution and the distribution in MIL-STD-210B based on the following equation from Tattelman and Sissenwine:

$$N(D) = 389\ R^{1.02} \exp\left[-3.67\, D/D_o\right] ,$$

where $D_o = 1.48\ R^{0.05}$.

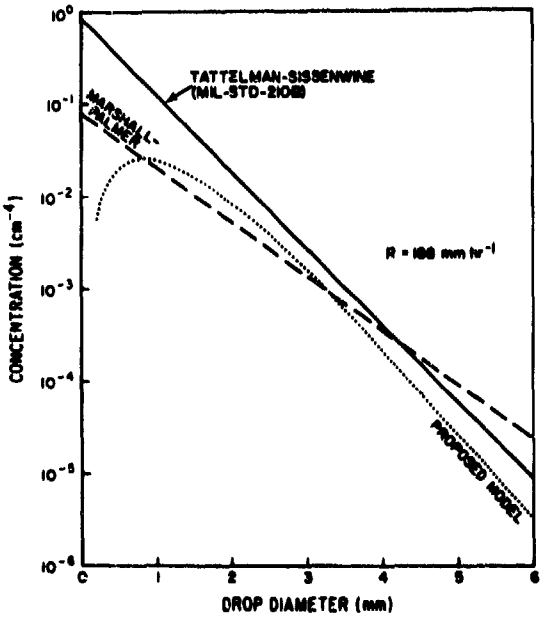

Figure 5. Comparison of the Gamma Function Model Fit With the Exponential Fits by Marshall-Palmer, and Tattelman and Sissenwine (MIL-STD-210B)

The integrated water content of the gamma distribution fit, up to a D_{max} of 6.5 mm, is 7.74 g/m^3 for this rate. The following empirical equation, used for MIL-STD-210B,

$$M = 0.052\ R^{0.97}$$

gives, as a comparison, a value of 8.35 g/m^3.

3.2.2 GOODNESS OF FIT

We now examine how well this model fits independently observed high rainfall rate data from Mueller and Sims,[11] as well as the high rate hurricane and tropical storm data on which it was based. Keep in mind that the model fit is not a tailored fit to each individual spectrum. The only input specified is either the rainfall rate or the water content. Figure 6 shows the fit to average distributions for three categories of rainfall rate for Miami, Florida. The fits are quite good to these spectra. The fit is particularly good for the highest rate category of 429 mm/hr.

Figure 7 presents the fit for average spectra from Majuro Atoll in the tropical Pacific for mean rain rates of 115 and 171 mm/hr. The fits are excellent, particularly for the 115 mm/hr rate spectrum. The same is true for the data from Bogor, Indonesia in Figure 8. The fit for the 125 mm/hr distribution is excellent, but for 180 mm/hr, the model underestimates the number concentration of drops of 1.5 mm diameter.

Figures 9 and 10 display the fit for the highest rate categories for two locations with more continental characteristics. The fit is generally quite good, but the model underestimates the concentrations at D = 1.5 mm and slightly overestimates the concentrations of the largest drops. Note that the Marshall-Palmer fit more severely underestimates concentrations at D = 1.5 mm and more severely overestimates the concentrations at D > 4 mm. The gamma distribution function model fits this independent set of high rainfall rate data quite well, particularly for locations within the tropics.

In Figures 1, 2, and 3, the model fit is compared with stratified subsets of the data on which it is based. The fits are quite good for this dependent data. For the data collected at a low sampling level (0.45 km), the overall fit is good, but the bimodal tendency previously noted in the most intense low level distributions does not lend itself well to a simple functional fit. Shiotsuki[17] presents several intense rainfall distributions that support this spectral shape for intense rainfall at the surface.

---

17. Shiotsuki, Y. (1976) An estimation of drop-size distribution in severe rainfall. J. Met. Soc. Japan 54:259-263.

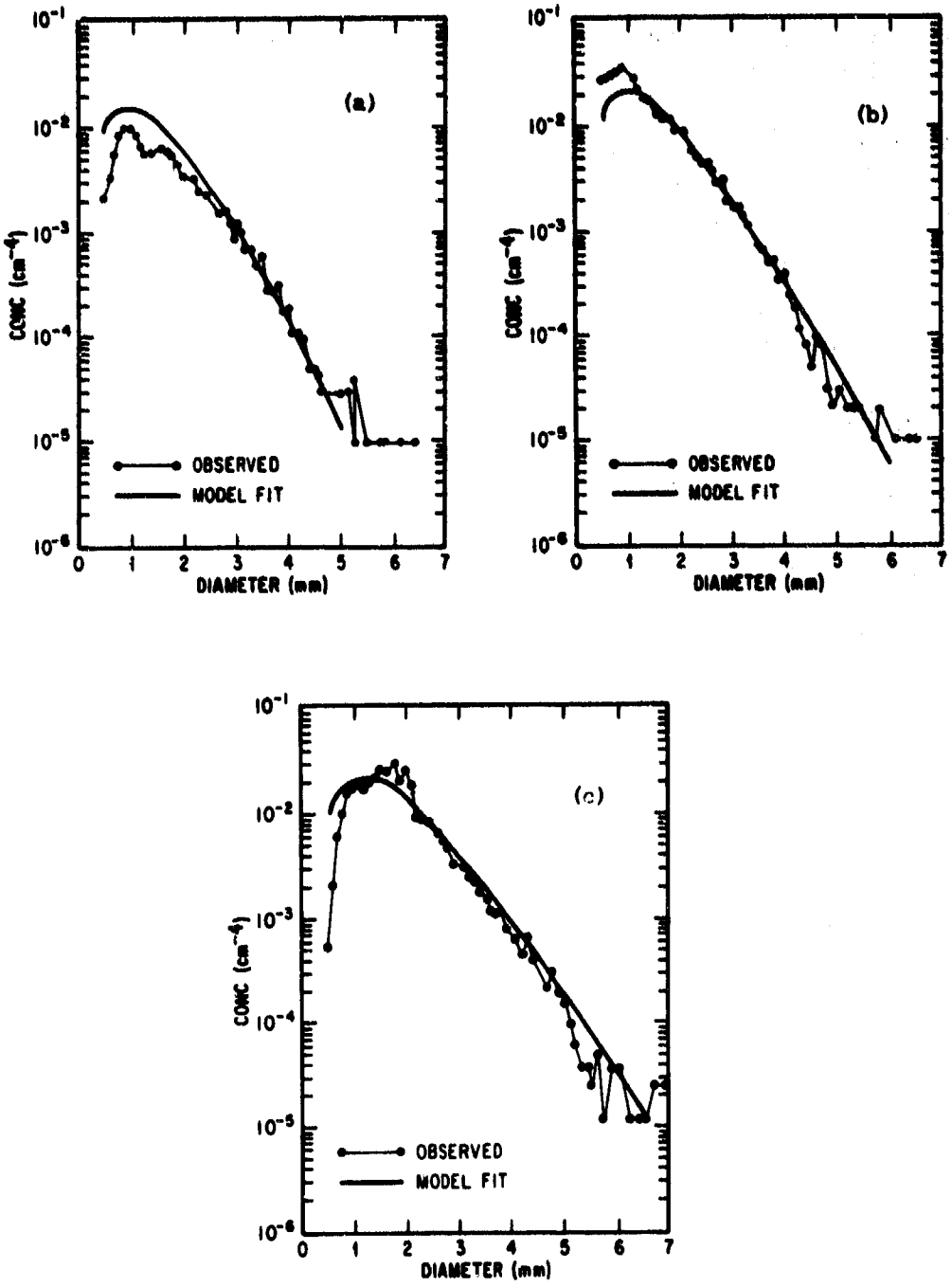

Figure 6. Model Fit Compared to Average Distributions at Miami, Florida for Rain Rates of: (a) 106 mm/hr, (b) 212 mm/hr, and (c) 429 mm/hr

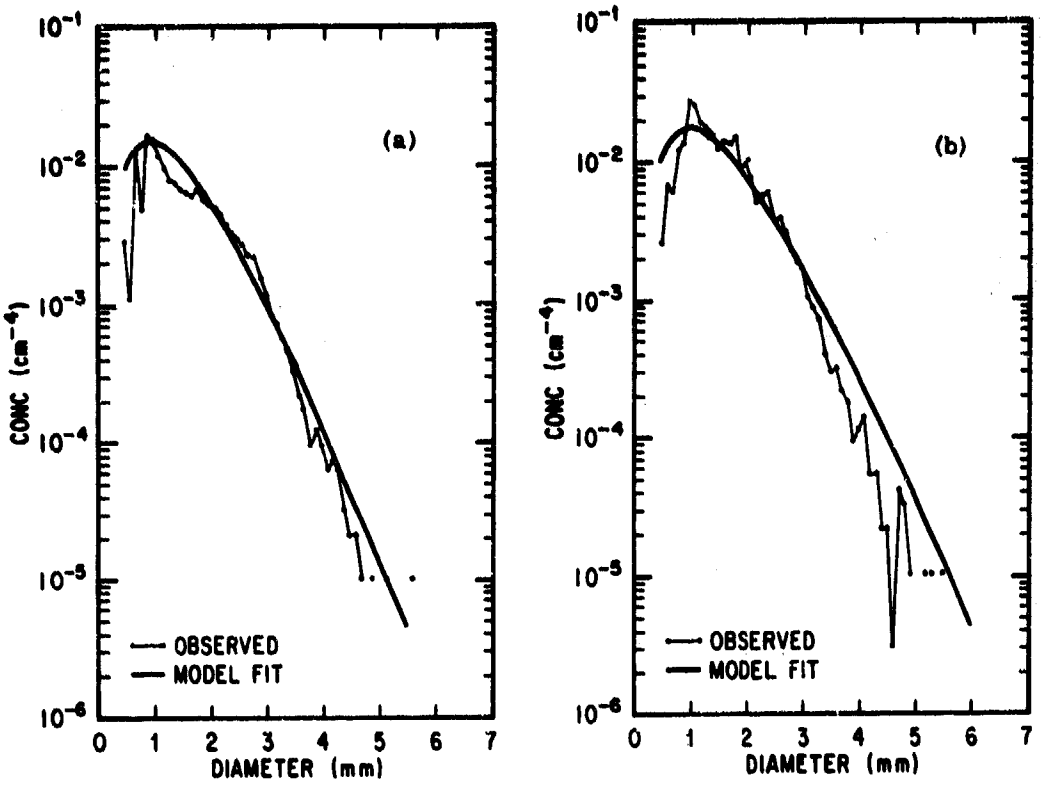

Figure 7. Model Fit Compared to Average Distributions at Majuro Atoll, Tropical Pacific, for Rain Rates of: (a) 115 mm/hr and (b) 171 mm/hr

3.3 Liquid Water Content

3.3.1 PRECIPITATION LIQUID WATER CONTENT

Measurements of liquid water content (M) in severe convective storms have not been made on a systematic basis,[18] however a value as high as 44 g/m^3 was reported by Roys and Kessler.[19] Their aircraft observations of maximum values in Oklahoma thunderstorms show that the next highest value was about 14 g/m^3, and the average of maximum amounts in 28 aircraft passes, including the 44 g/m^3 value, was 8.4 g/m^3. Kyle and Sand[20] found total condensed water contents of about 20 g/m^3 in "High Plains" thunderstorms. Mueller and Sims observed peak 10.5-sec values of 22 and 29 g/m^3 at the surface in Miami.

---

18. Grantham, D. D. et al (1983) Water vapor, precipitation clouds and fog: Chapter 16, 1983 Revision, Handbook of Geophysics and Space Environments. AFGL-TR-83-0181, AD A144176, 141 pp.

19. Roys, G. P., and Kessler, E. (1966) Measurements by Aircraft of Condensed Water in Great Plains Thunderstorms, ESSA Tech Note 49-NSSP-19.

20. Kyle, T.G., and Sand, W. R. (1973) Water content in convective storm clouds, Science, 180:1274-1276.

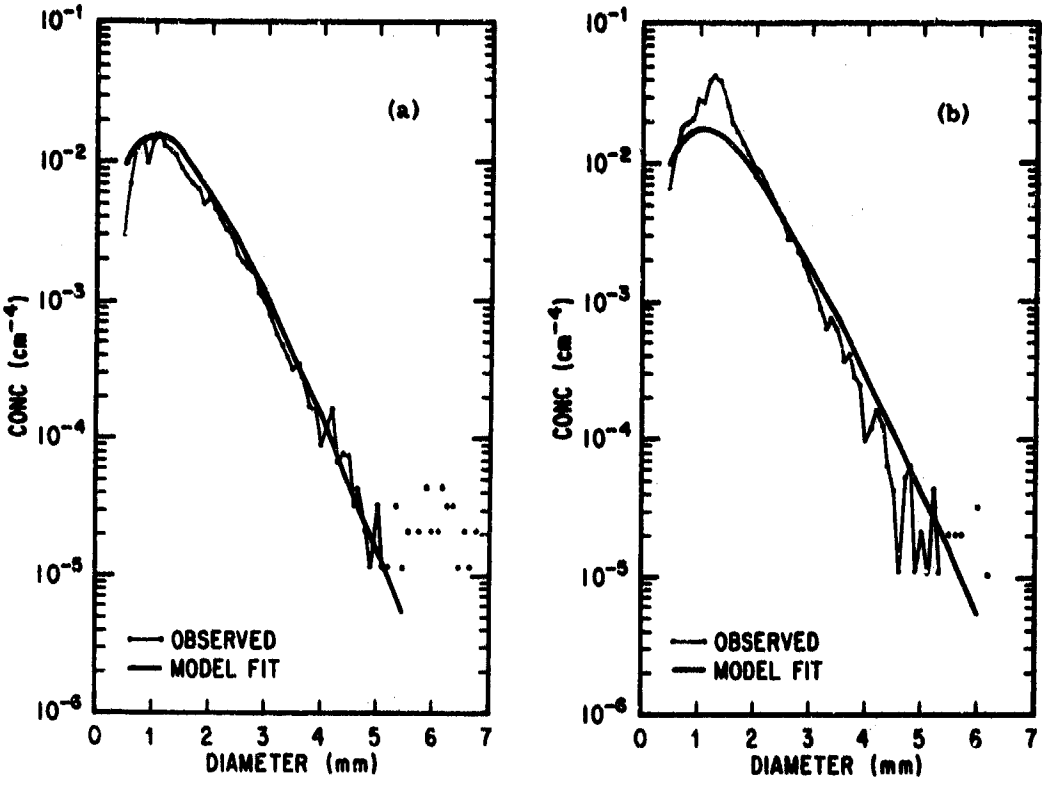

Figure 8. Model Fit Compared to Average Distributions at Bogor, Indonesia for Rain Rates of: (a) 125 mm/hr and (b) 180 mm/hr

Extreme values of rain rate, R, and M have been found to be fairly well described by a log-normal distribution. Such a distribution for the total sample of hurricane/tropical storm data analyzed for this study, and the sample for hurricane Eloise (1965), is shown in Figure 11. The ordinate is the conditional probability, (that is, R > 0). About 1 percent of the almost 14,000 ten-sec aircraft-track samples had a value of M greater than 4 g/m^3. For comparison, surface data from Mueller and Sims[11] are also shown, as are the Roys and Kessler data (excluding the 44 g/m^3 value). Note that the Roys and Kessler data are for maximum water content within Oklahoma thunderstorms.

The Mueller and Sims data cover a one-year period at Miami, Florida, Franklin, North Carolina, and Mujuro Atoll. Data for Bogor, Iodonesia was omitted for clarity, as it is coincident with the distribution of the data from this study. All of the distributions are very close to the data sample of this study, except possibly Miami, where the slope is the same but the curve is shifted. Note that the Roys and Kessler distribution changes quite radically at about 5 g/m^3, and the high water content values exhibit a significantly different slope than the data of this study and the Mueller and Sims data. Keep in mind that these data were sampled at the -30°C level in Oklahoma thunderstorms. At this level in these

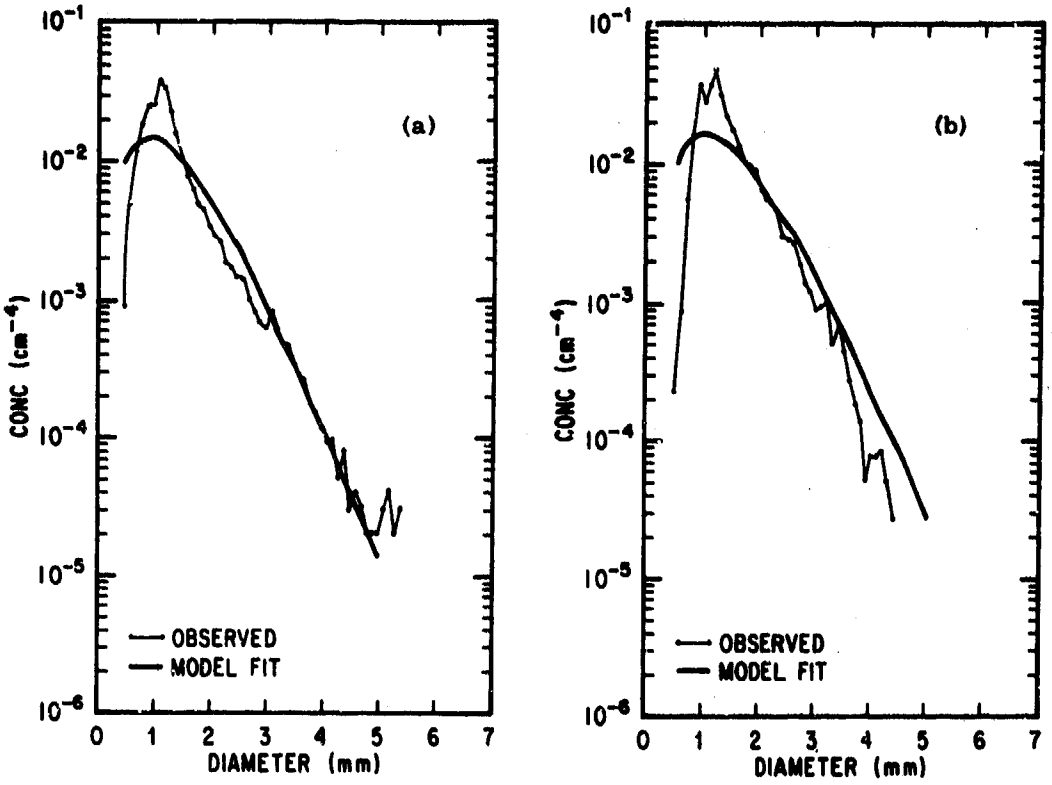

Figure 9. Model Fit Compared to Average Distributions at Island Beach, New Jersey for Rain Rates of: (a) 101 mm/hr and (b) 148 mm/hr

storms they could have been looking at accumulations of graupel, and not simply rain water content. This could explain the slope and the departure from log normality.

The liquid water content contained in precipitation size drops can be computed from the drop-size distribution, as well as the rainfall rate. This mass of water per cubic meter of air space is important for many applications and actually is a more fundamental parameter of the distributions than the rainfall rate. It is related to the rainfall rate, since R and M are proportional to $\sum v D^3$ and $\sum D^3$, respectively. The drop terminal velocity is not a strong function of drop diameter, particularly at large diameters.

Table 1 summarizes several empirical relationships between liquid water content and rainfall rate.

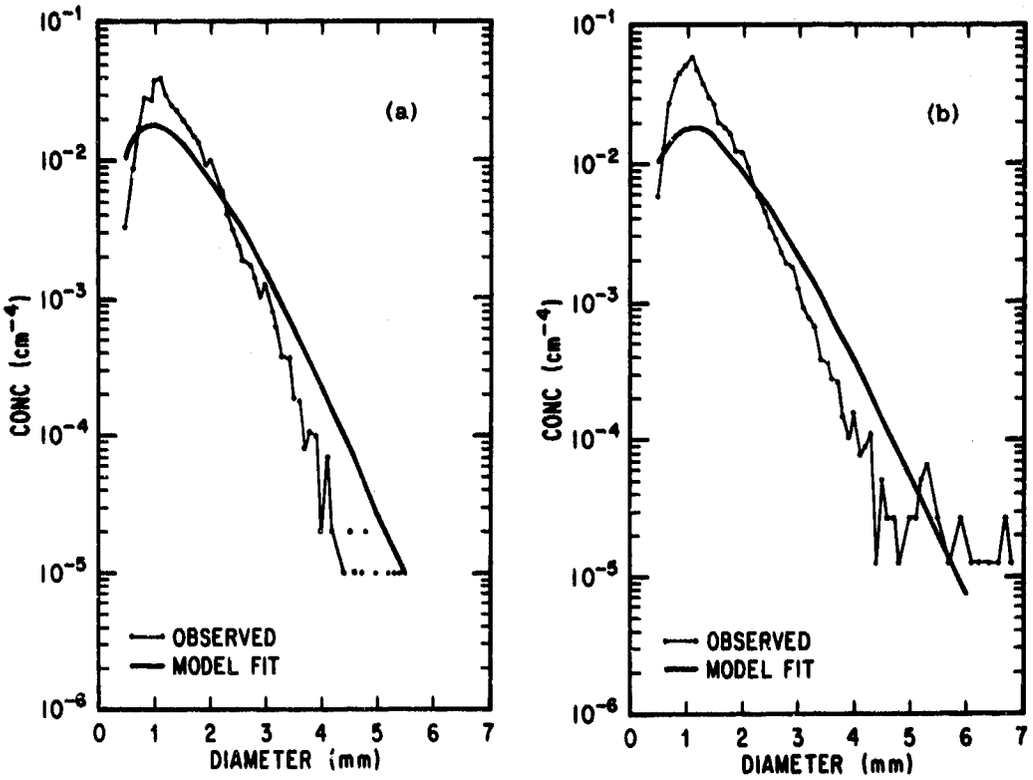

Figure 10. Model Fit Compared to Average Distributions at Franklin, North Carolina for Rain Rates of: (a) 144 mm/hr and (b) 205 mm/hr

Table 1. Empirical R vs M Relationships

Marshall-Palmer	$M = 0.072\ R^{0.88}$
Illinois (Sissenwine[2])	$M = 0.052\ R^{0.97}$
Tropical (Willis[14])	$M = 0.062\ R^{0.913}$
Florida (Mueller & Sims[11])	$M = 0.053\ R^{0.95}$

The Illinois thunderstorm equation was used by Sissenwine for inputs to MIL-STD-210B.

3.3.2 CLOUD LIQUID WATER CONTENT

A distinction should be made between precipitation water content and cloud droplet water content. A diameter of 100 μm is typically the boundary between the two categories of hydrometeors. This is also the lower size threshold of the precipitation probe that measured the size-distributions which were used to derive the model fit in Section 3.2.1. The MIL-STD-210B supporting material[2] stated

that the highest measured value of cloud water content, unquestionably composed of only cloud droplets (D < 100 μm), was about 6.5 g/m^3. This is in agreement with maximum adiabatic cloud liquid water contents. For MIL-STD-210B, a maximum cloud water content of 2.5 g/m^3 was added to the precipitation water contents for the least intense model of convective precipitation. This quantity was extrapolated upward to 10 g/m^3 for the more intense models.

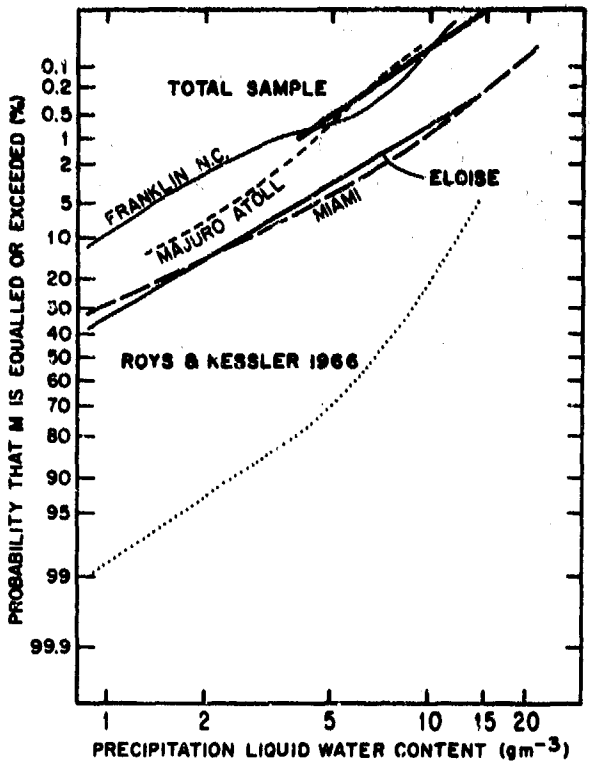

Figure 11. Log-normal Fit of Precipitation Water Content vs Conditional Probability (R > 0) of Being Exceeded for the Indicated Data Sources

Note that very high values of precipitation water content (10 g/m^3), and very high values of cloud droplet water content, are mutually exclusive and cannot co-exist. This is because the collection of small cloud droplets by the precipitation droplets is effective and rapid. For the typical raindrop spectrum associated with a precipitation water content of about 10 g/m^3, the time to completely sweep the volume of cloud droplets is approximately 30 sec or less. Even a very strong

updraft cannot supply 10 g/m^3 every 30 sec. Consequently, the cloud water content must level off, or go down, as the precipitation water content increases to extreme values. The collision breakup processes, which are really responsible for shaping the drop spectrum, are well developed in extreme rate distributions. The demarcation between cloud droplets and precipitation drops is in the range where collision breakup is supplying droplets. Nevertheless, the sweepout is so rapid and efficient that the water contents in the cloud droplet range cannot coexist with high precipitation water contents. Therefore, values of cloud water during extreme precipitation rates in MIL-STD-210B are considered unrealisticly high. For extreme rain-rate environments, the maximum cloud water content should not exceed 4 g/m^3.

3.4 Variation with Altitude

The distributions of hydrometeors with altitude in MIL-STD-210B, developed by Sissenwine,[2] are largely based on the profiles of Briggs.[21] Sissenwine increases the precipitation rate, and the precipitation water content, gradually from the surface to 4.5 km, holds it constant to 6.0 km, then gradually decreases it to near zero at 18 km. This is a compromise to at least partially include the radar profiles that show an "accumulation zone" maximum just above the freezing level at 4-6 km. However, this accumulation zone would not be operative at the same time that high rates are occurring at the surface. The evidence presented in this section indicates that a constant precipitation water content from the surface to 6 km is more realistic. The wide range of the ratios of intensity at altitudes above this maximum intensity to intensity at the surface is left as a topic for further investigation.

3.4.1 LIQUID WATER

There are two considerations with regard to vertical profiles of precipitation intensity and liquid water content which should be mentioned here. First, because of decreasing air density with altitude, the precipitation rate for a given drop-size distribution increases with altitude. In this report, profiles of precipitation rate with altitude are presented in terms of equivalent surface rate, not the actual rate at altitude. This was also done for MIL-STD-210B. The actual rate at altitude can be found by applying the density correction $(\rho_o/\rho)^{0.4}$ to the surface terminal velocities used to compute the rainfall rate from the drop-size distribution.[22]

---

21. Briggs, J. (1972) Probabilities of aircraft encounters with heavy rain, Met. Mag. 101(No. 1194):8-13.

22. Foote, G.B., and Dutoit, P.S. (1969) Terminal velocity of raindrops aloft, J. Appl. Meteor. 8:249-253.

Second, there is a great difference in the vertical profile of water content, at least at certain stages of development of the cloud, between a tropical convective cloud where warm rain processes are dominant through a deep bottom layer of the cloud, and a "High Plains" continental thunderstorm where the precipitation is initiated and grown almost exclusively in the ice phase. It is the latter case where the profile is likely to be of the accumulation zone type with an elevated hydrometeor maximum at an altitude of 4-6 km. Of course, there is a broad spectrum of conditions in between where both processes are operative. Accumulation of hydrometeors can occur with either process dominant when there is a reversal in the updraft velocity profile, which typically occurs in the upper parts of a convective cloud.

Figure 12 shows a vertical reflectivity and cloud water content profiles from passes through hurricanes.[23] Note that the reflectivity, indicative of precipitation rate, stays essentially constant, or decreases slightly, from the surface to the freezing level near 6 km. Figure 13 is a composite of vertical reflectivity profiles from several sources.[24] Generally, these profiles either stay relatively constant or decrease with altitude to about 5 km. The exceptions to this are the profiles, after Donaldson,[25] labeled "Hail" and "Tornado". These are probably typical of the accumulation zone type profiles, while the rest are typical of profiles where warm rain precipitation processes are well developed.

A distinction needs to be made between the vertical profile of precipitation water and the vertical profile of cloud water. For the intense rain conditions under consideration here, the precipitation processes are well developed in the cloud systems involved. In tropical convective clouds, the profile of Johnson-Williams measured cloud water content, presented in Figure 12, is typical. This instrument measures the liquid water contained in droplets of $D < 45$ μm, less than our cutoff definition of $D = 100$ μm. In intense tropical convection we typically find fairly low, nearly constant, cloud water contents from near cloud-base levels to above the freezing level, and then rapidly decreasing values above about 6 km. However, the profiles specified in MIL-STD-210B do not decrease it to low values quite so rapidly above 6 km. We subscribe to a gradual decrease in cloud water above 6 km for the model profiles developed in this report, primarily because our demarcation of 100 μm is in the breakup-fragment range. That is, fragmenting precipitation drops will, in effect, produce cloud-sized particles. The vertical profile of cloud water specified is very close to that of Sissenwine, albeit lower in magnitude.

---

23. Jorgensen, D. R. (1984) Mesoscale and Convective Scale Characteristics of Mature Hurricanes, Phd Thesis, Colorado State University, Fort Collins, Colorado, 189 pp.

24. Szeke, E. J., Zipser, E. J., and Jorgensen, D. P. (1985) A radar study of convective cells in mesoscale systems in GATE, Part I: Vertical profile statistics and comparison with hurricane cells, J. Atmos. Sci. To appear in a forthcoming issue.

25. Donaldson, R. J., Jr. (1961) Radar reflectivity profiles in thunderstorms. J. Meteor. 18:292-305.

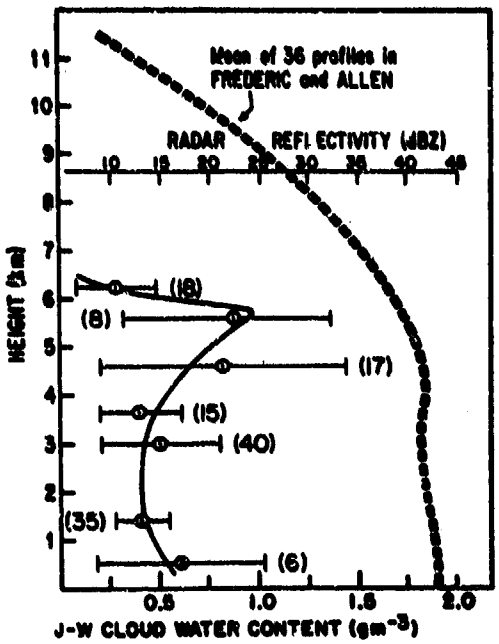

Figure 12. Mean Vertical Profiles of Cloud Water Content (measured by Johnson-Williams cloud water meter), and Radar Reflectivity, From a Vertically Scanning X-band Tail Radar. The J-W results are from passes through the eyewall of four mature hurricanes. The number of passes at each level are indicated in parenthesis. The reflectivity profile is a composite of eyewall passes of 2 hurricanes (from Jorgensen[23])

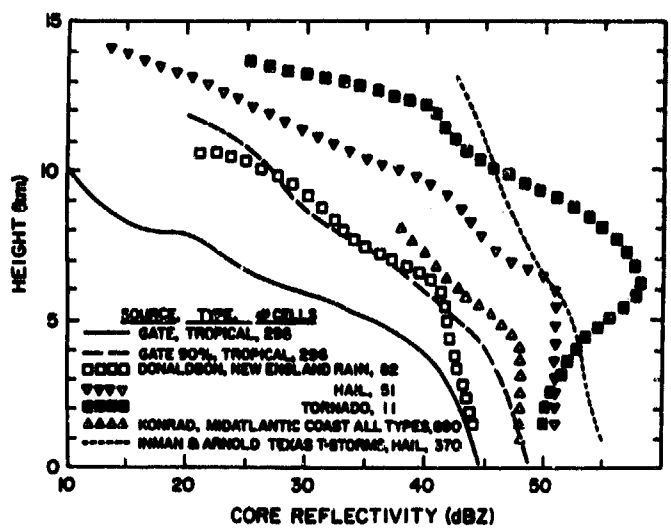

Figure 13. Vertical Reflectivity Profiles for the Indicated Data Sources (from Szoke et al[24])

3.4.2 TRANSITION TO ICE

The drop size distributions specified in the Standard extend to levels well above the level where solid-state precipitation becomes a factor, yet we have addressed only rain drop-size distributions. A typical freezing level for convective clouds that are producing very high precipitation rates is 4.5 km for a midwest thunderstorm, and is about 6 km in the warm parts of a hurricane, as an extreme case for the tropics.

The transition to ice tends to be somewhat different for tropical convection than for more continental mid-latitude convection. In tropical convective clouds the transition to all ice is rapid and is essentially complete by -10° C or about 7 km. So, for these clouds the precipitation should be considered to be completely liquid below 4.5 km (although some very large graupel may survive to lower warmer levels), and to be a mixture of water and ice which is becoming predominantly ice with increasing altitude between 4.5 and 7 km, and to be all ice above about -10° C or 7 km. For more continental clouds the mixture can start at slightly lower levels and the mixture can extend higher above the freezing level, but the mixture consists of cloud water and ice, not raindrops and ice.

The mixture of high concentrations of liquid water contained in large precipitation sized drops and ice is practically nonexistent above the freezing level. In simplified terms, we can consider condensed water in convective clouds to be comprised of two liquid water distributions—high number density small droplet cloud water and low number density rain water, and two ice distributions—low number density large ice (large graupel and hail), and high number density small ice (ice crystals and snow). There are four combinations of ice and water which are possible. In two of these an ice and water mixture can only exist as a transient feature. Small ice and rainwater cannot coexist because the falling raindrops will quickly contact a small ice particle and freeze. High concentrations of small ice and cloud water cannot coexist because the ice will quickly grow at the expense of the cloud water. Cloud water and low concentrations of large ice can coexist. Low concentrations of large ice and rainwater can coexist, but this combination is not likely above the freezing level, although it is common below.

For the profiles derived herein, the precipitation should be considered all liquid below 4.5 km, then a mixture of water and ice becoming all ice above about -10° C or 7 km. This is in contrast with the mix of water and ice up to 10 km in MIL-STD-210B. The model size distributions should be considered as roughly equivalent water distributions, even though this is not strictly correct.

3.4.3 HAIL

Hail is, of course, a possibility in intense convective clouds, although more likely in mid-latitudes than in the tropics. Intense tropical convective clouds do not typically have graupel particles much above about 1 cm. When dry air intrusions and extreme instabilities are involved, as is the rule rather than the exception for intense mid-latitude convective storms, hail becomes a prime consideration. Although the models derived here extend through hail altitudes, hail distributions are covered in a separate part of the Standard.

4. MODEL PROFILES OF HYDROMETEOR EXTREMES

Using the above rationale, model hydrometeor profiles were developed based on five surface rainfall rates, 36, 84, 168, 432, and 1872 mm/hr. The first three rates correspond to the 0.5 percent, 0.1 percent, and 0.01 percent worst month frequency of occurrence in the most severe area of the world. The last two are the 42- and 1-min world record rainfalls, respectively. The precipitation water content was kept to constant to 6 km, then decreased gradually to zero at 20 km. The decrease above 6 km was kept nearly the same as that in MIL-STD-210B. Although the true cloud water content, that is, the water content due to cloud forming processes, decreases as the rain rate increased to extreme values, the D = 100 μm cutoff definition of cloud water puts it in a range where the collision breakup of larger drops introduces significant amounts of water in collision fragments. Consequently, a peak cloud water content of 2.5 g/m^3 is specified for the 36 mm/hr distribution, then this content is increased to 4 g/m^3 for the 168 mm/hr distribution and kept constant there for the two highest rates. The shape of the vertical profile is kept the same as the profiles specified in the previous standard. The vertical profile shapes for cloud water and precipitation water content are summarized in Table 2.

The equations for the model distributions for the five surface rainfall rates are:

36 mm/hr $\quad N(D) = 45.08D^{2.160} \exp[-32.75D]$ (12)

84 $\quad N(D) = 43.86D^{2.160} \exp[-28.76D]$ (13)

168 $\quad N(D) = 42.88D^{2.160} \exp[-25.86D]$ (14)

432 $\quad N(D) = 41.59D^{2.160} \exp[-22.37D]$ (15)

1872 $\quad N(D) = 39.66D^{2.160} \exp[-17.86D]$ (16)

where N(D) is in cm^{-4} and D in cm. Thus, to find the concentrations per m^3 in a 0.1 mm diameter size interval, N(D) in cm^{-4} must be multiplied by 1×10^4.

Table 2. Vertical Profile Shapes for Cloud and Precipitation Water

Altitude km	Ratios	
	Precip	Cloud
0	1.00	0
2	1.00	0.86
4	1.00	0.97
6	1.00	1.00
8	0.74	0.68
10	0.51	0.47
12	0.35	0.32
14	0.22	0.19
16	0.11	0.10
18	0.03	0.02
20	0.00	0.00

The drop-size distributions for the model hydrometeor profiles are presented as the number of drops per 1-mm size interval of the drop diameters up to a maximum of 6.49 mm. The number for each 1-mm size range was calculated by summing the number of drops per 0.1 mm size range and then rounding to the nearest whole drop. As in MIL-STD-210B, a small end cutoff of 0.5 mm is used for the drop-size distributions. The hydrometeor profiles are tabulated from the surface to 20 km in Tables 3-7.

There are indications that the gamma fit model may break down for extreme rates such as the world record 1872 mm/hr. The collision breakup processes may make the distributions bimodal and tend to shift the peak of the distribution to larger drop diameters. However, based on the data of this study, the extrapolation of the gamma fit to these rates is reasonable.

In Section 3.4 we discussed the existence of an accumulation zone wherein an elevated hydrometeor maximum exists at 4 to 6 km. For design problems where a very low risk of failure is required (for example, engine flameout), more extreme

values of water content than those indicated for the least intense profiles should be considered. Extreme observed water contents are discussed in Section 3.3

Figure 14 summarizes the contribution to the total precipitation water content of each 0.5 mm diameter interval for rainfall rates of 36 and 432 mm/hr. The distributions from which this was calculated are the model fits for these rainfall rates. Note the very small contribution from drops < 0.5 mm in diameter. Of course this is underestimated slightly because the fit underestimates the concentration in these small drops as discussed in Section 3.2 The shift of the major contribution to larger drop sizes, consistent with the increase in median volume diameter of the distribution, is evident.

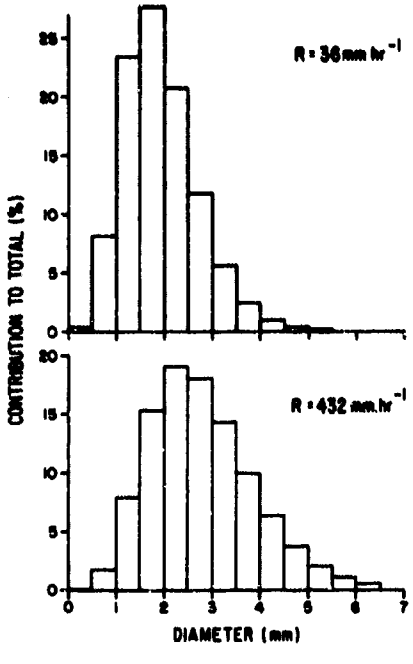

Figure 14. The Contribution to the Total Precipitation Water Content of each 0.5-mm Diameter Interval for Rainfall Rates of 36 and 432 mm/hr

Table 3. Model Hydrometeor Profile Based on a Surface Rainfall Rate of 36 mm/hr

Altitude (km)	Rainfall Rate (mm/hr)	Median Volume Diameter (mm)	Precip Water (g/m^3)	Cloud Water (g/m^3)	Drop Concentrations (per m^3) in 1-mm Size Intervals Diameter (mm)					
					0.5-1.4	1.5-2.4	2.5-3.4	3.5-4.4	4.5-5.4	5.5-6.4
0	36.0	1.71	1.6	0	1154	260	26	2	< 1	< 1
2	36.0	1.71	1.6	2.1	1154	260	26	2	< 1	< 1
4	36.0	1.71	1.6	2.4	1154	260	26	2	< 1	< 1
6	36.0	1.71	1.6	2.5	1154	260	26	2	< 1	< 1
8	26.6	1.63	1.2	1.7	1017	199	17	1	< 1	0
10	18.4	1.54	0.9	1.2	864	141	10	< 1	< 1	0
12	12.6	1.45	0.6	0.8	728	98	6	< 1	< 1	0
14	7.9	1.35	0.4	0.5	583	60	3	< 1	0	0
16	4.0	1.22	0.2	0.2	409	28	< 1	< 1	0	0
18	2.9	1.16	0.2	0.1	345	19	< 1	< 1	0	0
20	0	0	0	0	0	0	0	0	0	0

Notes:

(1) All rain rates are surface equivalent intensities. See Section 3.4.1 to determine actual intensity for a given altitude

(2) Distributions are all liquid below 4.5 km, mostly liquid 4.5-6.0 km and nearly all ice above 7.0 km. Numbers are in terms of equivalent raindrops for solid precipitation.

(3) Cloud-Precipitation water division at D = 100 μm. Cloud water includes ice with melted diameters D < 100 μm.

Table 4. Model Hydrometeor Profile Based on a Surface Rainfall Rate of 84 mm/hr

Altitude (km)	Rainfall Rate (mm/hr)	Median Volume Diameter (mm)	Precip. Water (g/m^3)	Cloud Water (g/m^3)	Drop Concentrations (per m^3) in 1-mm Size Intervals Diameter (mm)					
					0.5-1.4	1.5-2.4	2.5-3.4	3.5-4.4	4.5-5.4	5.5-6.4
0	84.0	1.94	3.5	0	1608	520	77	8	< 1	< 1
2	84.0	1.94	3.5	3.0	1608	520	77	8	< 1	< 1
4	84.0	1.94	3.5	3.4	1608	520	77	8	< 1	< 1
6	84.0	1.94	3.5	3.5	1608	520	77	8	< 1	< 1
8	62.2	1.86	2.7	2.4	1435	410	53	5	< 1	< 1
10	42.8	1.75	1.9	1.7	1239	302	33	3	< 1	< 1
12	29.4	1.65	1.4	1.1	1060	218	20	1	< 1	0
14	18.5	1.54	0.9	0.7	867	142	10	< 1	< 1	0
16	9.2	1.38	0.5	0.4	628	71	3	< 1	0	0
18	6.7	1.32	0.4	0.1	537	51	2	< 1	0	0
20	0	0	0	0	0	0	0	0	0	0

Notes:

(1) All rain rates are surface equivalent intensities. See Section 3.4.1 to determine actual intensity for a given altitude.

(2) Distributions are all liquid below 4.5 km, mostly liquid 4.5-6.0 km and nearly all ice above 7.0 km. Numbers are in terms of equivalent raindrops for solid precipitation.

(3) Cloud-Precipitation water division at D = 100 μm. Cloud water includes ice with melted diameters D < 100 μm.

Table 5. Model Hydrometeor Profile Based on a Surface Rainfall Rate of 168 mm/hr

Altitude (km)	Rainfall Rate (mm/hr)	Median Volume Diameter (mm)	Precip. Water (g/m^3)	Cloud Water (g/m^3)	Drop Concentrations (per m^3) in 1-mm Size Intervals Diameter (mm)					
					0.5-1.4	1.5-2.4	2.5-3.4	3.5-4.4	4.5-5.4	5.5-6.4
0	168.0	2.16	6.7	0	2057	863	170	25	3	< 1
2	168.0	2.16	6.7	3.4	2057	863	170	25	3	< 1
4	168.0	2.16	6.7	3.9	2057	863	170	25	3	< 1
6	168.0	2.16	6.7	4.0	2057	863	170	25	3	< 1
8	124.3	2.06	5.1	2.7	1853	696	122	16	2	< 1
10	85.7	1.95	3.6	1.9	1620	528	79	9	< 1	< 1
12	58.8	1.84	2.6	1.3	1404	392	50	5	< 1	< 1
14	37.0	1.71	1.7	0.8	1166	266	27	2	< 1	< 1
16	18.5	1.54	0.9	0.4	867	142	10	< 1	< 1	0
18	13.4	1.47	0.7	0.1	750	104	6	< 1	< 1	0
20	0	0	0	0	0	0	0	0	0	0

Notes:

(1) All rain rates are surface equivalent intensities. See Section 3.4.1 to determine actual intensity for a given altitude.

(2) Distributions are all liquid below 4.5 km, mostly liquid 4.5-6.0 km and nearly all ice above 7.0 km. Numbers are in terms of equivalent raindrops for solid precipitation.

(3) Cloud-Precipitation water division at D = 100 μm. Cloud water includes ice with melted diameters D < 100 μm.

Table 6. Model Hydrometeor Profile Based on a Surface Rainrall Rate of 432 mm/hr

Altitude (km)	Rainfall Rate (mm/hr)	Median Volume Diameter (mm)	Precip. Water (g/m^3)	Cloud Water (g/m^3)	Drop Concentrations (per m^3) in 1-mm Size Intervals Diameter (mm)					
					0.5-1.4	1.5-2.4	2.5-3.4	3.5-4.4	4.5-5.4	5.5-6.4
0	432.0	2.50	15.8	0	2779	1595	440	91	16	3
2	432.0	2.50	15.8	3.4	2779	1595	440	91	16	3
4	432.0	2.50	15.8	3.9	2779	1595	440	91	16	3
6	432.0	2.50	15.8	4.0	2779	1595	440	91	16	3
8	319.7	2.39	12.0	2.7	2535	1323	329	61	10	1
10	220.3	2.25	8.5	1.9	2251	1038	226	37	5	< 1
12	151.2	2.13	6.1	1.3	1984	801	151	21	3	< 1
14	95.0	1.98	4.0	0.8	1683	571	89	10	1	< 1
16	47.5	1.78	2.1	0.4	1291	329	38	3	< 1	< 1
18	34.6	1.70	1.6	0.1	1135	251	25	2	< 1	< 1
20	0	0	0	0	0	0	0	0	0	0

Notes:

(1) All rain rates are surface equivalent intensities. See Section 3.4.1 to determine actual intensity for a given altitude.

(2) Distributions are all liquid below 4.5 km, mostly liquid 4.5-6.0 km and nearly all ice above 7.0 km. Numbers are in terms of equivalent raindrops for solid precipitation.

(3) Cloud Precipitation water division at D = 100 μm. Cloud water includes ice with melted diameters D < 100 μm.

Table 7. Model Hydrometeor Profile Based on a Surface Rainrall Rate of 1872 mm/hr

Altitude (km)	Rainfall Rate (mm/hr)	Median Volume Diameter (mm)	Precip. Water (g/m^3)	Cloud Water (g/m^3)	Drop Concentrations (per m^3) in 1-mm Size Intervals Diameter (mm)					
					0.5-1.4	1.5-2.4	2.5-3.4	3.5-4.4	4.5-5.4	5.5-6.4
0	1872.0	3.13	60.3	0	4121	3547	1514	487	135	34
2	1872.0	3.13	60.3	3.4	4121	3547	1514	487	135	34
4	1872.0	3.13	60.3	3.9	4121	3547	1514	487	135	34
6	1872.0	3.13	60.3	4.0	4121	3547	1514	487	135	34
8	1385.3	2.99	45.8	2.7	3826	3052	1200	356	90	21
10	954.7	2.82	32.6	1.9	3475	2511	888	236	54	11
12	655.2	2.66	23.1	1.3	3135	2037	643	152	31	6
14	411.8	2.48	15.1	0.8	2739	1549	420	85	15	2
16	205.9	2.23	8.0	0.4	2202	992	211	33	5	< 1
18	149.7	2.12	6.0	0.1	1978	796	150	21	3	< 1
20	0	0	0	0	0	0	0	0	0	< 0

Notes:

(1) All rain rates are surface equivalent intensities. See Section 3.4.1 to determine actual intensity for a given altitude.

(2) Distributions are all liquid below 4.5 km, mostly liquid 4.5-6.0 km and nearly all ice above 7.0 km. Numbers are in terms of equivalent raindrops for solid precipitation.

(3) Cloud-Precipitation water division at D = 100 μm. Cloud water includes ice with melted diameters D < 100 μm.

5. SUMMARY

Model hydrometeor profiles, from the surface to 20 km, were developed based on five surface rainfall rates, 36, 84, 168, 432, and 1872 mm/hr. The first three rates correspond to the 0.5 percent, 0.1 percent, and 0.01 percent frequency of occurrence during the worst month in the most severe area of the world. The last two are the 42- and 1-min world record rainfalls, respectively.

A large sample of drop-size distributions from intense rainfall in tropical convection was analyzed. A gamma distribution function was fit to the normalized set of intense rainfall drop-size distributions. This fit formed the basis of a model distribution as a function of rainfall rate or precipitation water content. The model fit was applied to numerous observed high rainfall rate drop-size distributions from several geographic locations and was found to very reasonably characterize these observed distributions.

This model was used to specify the profiles of drop-size distributions for five categories of intense rainfall. The additional data considered in this study provide an improved specification of drop-size distributions for intense rainfall.

References

1. Department of Defense (1973) Military Standard, Climatic Extremes for Military Equipment, MIL-STD-210B, 15 December 1973, Office of the Under Secretary of Defense, Research and Engineering, Washington, D. C.
2. Sissenwine, N. (1972) Extremes of Hydrometeors at Altitude for MIL-STD-210B, AFCRL-TR-72-0369, AD 747482.
3. Tattelman, P., and Sissenwine, N. (1973) Extremes of Hydrometeors at Altitude for MIL-STD-210B, Supplement Drop-size Distributions, AFCRL-TR-73-0008, AD 756832.
4. Salmela, H.A., Sissenwine, N., and Lenhard, R.W. (1971) Preliminary Atlas of 1.0, 0.5, and 0.1 Percent Precipitation Intensities for Eurasia, AFCRL-TR-71-0527, AD 736406.
5. Tattelman, P., and Scharr, K.G. (1983) A model for estimating one-minute rainfall rates, J. of Climate and Appl. Meteor. 22:1575-80.
6. Tattelman, P., and Grantham, D.D. (1983) Northern Hemisphere Atlas of 1-Min Rainfall Rates, AFGL-TR-83-0267, AD A145411.
7. Tattelman, P., and Grantham, D.D. (1983) Southern Hemisphere Atlas of 1-Min Rainfall Rates, AFGL-TR-83-0285, AD A145421.
8. Knollenberg, R.G. (1981) Techniques for Probing Cloud Microstructure. Clouds, Their Formation, Optical Properties and Effects, P.V. Hobbs and A. Deepak, Eds., Academic Press, 15-92.
9. Jorgensen, D.P., and Willis, P.T. (1982) A Z-R relationship for hurricanes, J. Appl. Meteor. 21:356-366.
10. Blanchard, D.C., and Spencer, A.T. (1970) Experiments on the generation of raindrop-size distributions by drop breakup. J. Atmos. Sci. 27:101-108.
11. Mueller, E.A., and Sims, A.L. (1966) Radar Cross Sections From Drop Size Spectra. Tech. Rep. ECOM-00032-F, Contract DA-28-043 AMC-00032(E) Illinois State Water Survey, Urbana, Illinois, 110 pp. [AD 645218].

12. Hudson, N.W. (1963) Raindrop size distribution in high intensity storm. Rhodesian J. Agric. Res., 1, 6-11 (quoted in Blanchard and Spencer, 1970).

13. Ulbrich, C.W. (1983) Natural variations in the analytical form of the raindrop size distribution, J. Appl. Meteor. 22:1764-1775.

14. Willis, P.T. (1984) Functional fits to some observed drop side distributions and parameterizations of rain. J. Atmos. Sci. 41:1648-1661.

15. Sekhon, R.S., and Srivastava, R.C. (1970) Snow size spectra and radar reflectivity, J. Atmos. Sci. 27:299-307.

16. Sekhon, R.S., and Srivastava, R.C. (1971) Doppler observations of drop size distributions in a thunderstorm. J. Atmos. Sci. 28:983-994.

17. Shiotsuki, Y. (1976) An estimation of drop-size distribution in severe rainfall. J. Met. Soc. Japan 54:259-263.

18. Grantham, D.D. et al (1983) Water vapor, precipitation, clouds and fog: Chapter 16, 1983 Revision, Handbook of Geophysics and Space Environments. AFGL-TR-83-0181, AD A144176, 141 pp.

19. Roys, G.P., and Kessler, E. (1966) Measurements by Aircraft of Condensed Water in Great Plains Thunderstorms, ESSA Tech Note 49-NSSP-19.

20. Kyle, T.G., and Sand, W.R. (1973) Water content in convective storm clouds, Science, 180:1274-1276.

21. Briggs, J. (1972) Probabilities of aircraft encounters with heavy rain, Met. Mag. 101(No. 1194):8-13.

22. Foote, G.B., and Dutoit, P.S. (1969) Terminal velocity of raindrops aloft, J. Appl. Meteor. 8:249-253.

23. Jorgensen, D.R. (1984) Mesoscale and Convective-Scale Characteristics of Mature Hurricanes, Phd Thesis, Colorado State University, Fort Collins, Colorado, 189 pp.

24. Szoke, E.J., Zipser, E.J., and Jorgensen, D.P. (1985) A radar study of convective cells in mesoscale systems in GATE, Part 1: Vertical profile statistics and comparison with hurricane cells, J. Atmos. Sci. To appear in a forthcoming issue.

25. Donaldson, R.J., Jr. (1961) Radar reflectivity profiles in thunderstorms. J. Meteor. 18:292-305.